

A Direct PWM Voltage Controller of MPPT & Sizing of DC Loads for Photovoltaic System

Original

A Direct PWM Voltage Controller of MPPT & Sizing of DC Loads for Photovoltaic System / Murtaza, Ali Faisal; Chiaberge, Marcello; Spertino, Filippo; Ahmad, Jawad; Ciocia, Alessandro. - In: IEEE TRANSACTIONS ON ENERGY CONVERSION. - ISSN 0885-8969. - ELETTRONICO. - 33:3(2018), pp. 991-1001. [10.1109/TEC.2018.2823382]

Availability:

This version is available at: 11583/2720587 since: 2020-01-27T23:22:59Z

Publisher:

Institute of Electrical and Electronics Engineers Inc.

Published

DOI:10.1109/TEC.2018.2823382

Terms of use:

This article is made available under terms and conditions as specified in the corresponding bibliographic description in the repository

Publisher copyright

(Article begins on next page)

A Direct PWM Voltage Controller of MPPT & Sizing of DC Loads for Photovoltaic System

Ali Faisal Murtaza, Marcello Chiaberge, Filippo Spertino, Jawad Ahmad, and Alessandro Ciocia

Abstract—In a photovoltaic (PV) system, the appropriate voltage regulation is essential to guarantee the maximum power operation. In this paper, a direct pulse width modulation controller based on a single gain (k) is presented. This controller directly estimates the duty cycle (D) through gain k , and simultaneously its mathematical operation contains the properties of integral controller. Initially, a comprehensive study is presented to evaluate the D values according to reference points on I–V curves with contrasted irradiance levels. This study has been carried out for resistive and battery loads. Based on critical observations, separate tuning expressions of k gain have been designed for resistive and battery loads. It is revealed that with regard to varying weather, k gain is dynamic for resistive load, while static for battery load. Moreover, it is also shown that inappropriate setting of load will limit maximum power point tracker controller to reach the MPP point. Therefore, two more expressions have been presented to configure the resistive and battery loads. Comparative analysis between different D-schemes is presented, which indicates that for both loads, the proposed scheme has the superior performance with less complexity. Finally, numerous experimental tests have been conducted to verify the tuning criteria and working principle of the proposed scheme.

Index Terms—Photovoltaic (PV), voltage regulation, maximum power point tracker (MPPT), gain tuning, DC loads.

I. INTRODUCTION

MAXIMUM power point tracking (MPPT) technique plays an indispensable role to ensure the optimal operation of Photovoltaic (PV) array [1]. In search of MPP under distinct weather conditions, MPPT methods work in coalition with dc-dc converter for adequate PV voltage (V_{pv}) regulation. The voltage regulation is executed through pulse width modulation (PWM) of duty cycle (D) of the converter [2]–[4]. Since every change in PWM of D corresponds to a waiting period of 5–50 ms [3], the execution duration of PWM controller is substantial as compared to MPPT algorithm. This is because

of second order transients of dc-dc converter [3]. Naturally, the PWM controller determines the tracking ability and dynamic efficiency of a PV system.

The output variable of the MPPT algorithm may serve as current reference (I_{Ref}) or voltage reference (V_{Ref}). However, controlling PV voltage (V_{pv}) is the preferred option because of superior stability and less prone to irradiance variations. In general, MPPT designers estimate the V_{Ref} of global maximum (GM) during partial shading conditions. MPPTs based on I–V curve tracer [3], voltage/region analysis [5]–[8], cuckoo search [9] and module voltage [10], [11], are some prominent examples of these methods. Moreover, in recent past, MPPT designers also employed the significant use of V_{Ref} for uniform conditions [12]–[14]. The scientific nature of these algorithms, though varies from simple to advanced intelligence concepts. However, as far as PWM is concerned, conventional controllers almost become de-facto standard for MPPT techniques owing to low maintenance cost and complexity.

The problem arises when conventional controllers face the I–V curves, which vary non-linearly with irradiance, temperature and load. Although a fixed gain controller can perform well under specific weather condition [15]; however, its performance decays abruptly for changing weather conditions. The compromised performance of traditional controllers is related to their static gain settings, which can be mitigated by making these controllers adaptive. It is also observed that these controllers may struggle to cover the entire voltage range due to inappropriate load setting [15].

Adaptive schemes based on model-reference [16], self-tuning regulator [17] and online frequency-response measurement [18] have been successfully applied to conventional controllers for dc-dc converter applications. However, the first real attempt to design an auto-tune PID controller for a PV system with appreciable results is presented in [15]. This method is developed through linearized model of PV and dc-dc converter. Moreover, polynomial curve-fitting mathematical model is used for parameter extraction. The main drawback of this method is its complexity and required advanced statistical concepts.

In another study [19], fictitious reference iterative tuning (FRIT) method is proposed for the optimization of controller gains. This FRIT is based on particle swarm optimization and other complex procedures, which makes the implementation cost of this method high. A linearized model based PI controller is proposed in [20], which regulates the power instead of voltage.

Work presented in [21], [22] designed highly advanced voltage controllers to enhance the transient performance of

traditional controllers. These schemes achieved excellent results for grid-connected system with small capacitor at the PV generator. The extensive mathematical modeling, tuning of multiple parameters, numerous sensors, at times prior training, and sophisticated embedded system (high crystal frequency) are the demands of these controllers. Naturally, these methods are expensive for low power PV applications and micro-grids, where each controller has its own PV module. Also, the designing is not discussed with regard to DC loads.

By keeping the focus on conventional PWM controllers, following shortcomings have been found after exhaustive literature survey:

- 1) The conventional controllers are made adaptive by the auto tuning of gains [15]. However, rigorous optimization procedures and extensive mathematical modeling are required. The regulators based on advanced schemes are also highly complex and expensive [20], [21].
 - As control action involves high frequency switching of dc-dc converter and fast varying weather conditions, a simple and one-step online auto-tuner algorithm is required.
- 2) Usually, the characteristics of controller are modeled with respect to voltage source, i.e., battery or input side of inverter etc [22]–[24]. By contrast, limited emphasis is given to resistive load for DC load applications.
 - Previous work failed to address the gain settings for distinct loads. For instance, if the gains are set for battery load, will they also be valid for resistive load?
- 3) Different types of loads produce distinct effects on the operating range of the controller. As a result, an inappropriate sizing of load may limit the controller to reach the MPP point [25].
 - Current studies though discuss these effects; however, mathematical relations for correct sizing of distinct loads are required that enables the full coverage of array voltage.

In view of aforementioned issues, this paper presents a single gain (k) based PWM controller to compute D for dc-dc converter. The proposed controller is a refined form of the proportional (P) controller; main contribution lies in the application and optimization of this controller according to PV system of any array size and load. Moreover, two new expressions are designed to configure the resistive and battery loads from this study.

Initially, a comprehensive study is presented with regard to correlation between duty cycle and loads (resistive and battery) with different weather conditions. This study is conducted to evaluate the adaptive or static nature of PWM controller. Thereafter, the controller is designed, the key features of which are:

- 1) The mathematical operation of the controller works with single gain, and still it holds the innate characteristics of integral controller.
- 2) For both resistive and battery loads, the controller is auto-tuned during each iteration by single step tuning relations of gain k .
- 3) The boundary limits of linear modulation index of D , i.e., $0 < D < 1$ are properly addressed.

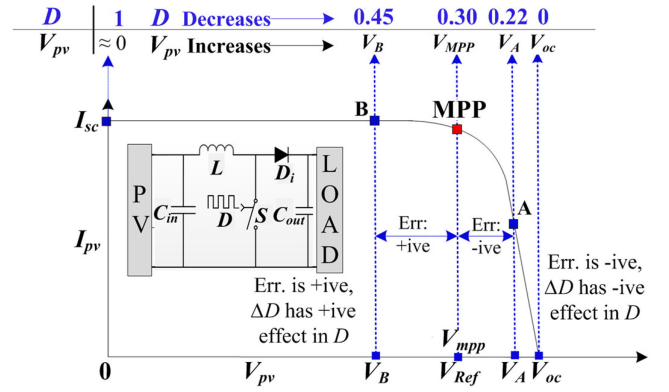


Fig. 1. Duty cycle and V_{pv} relation of PV array.

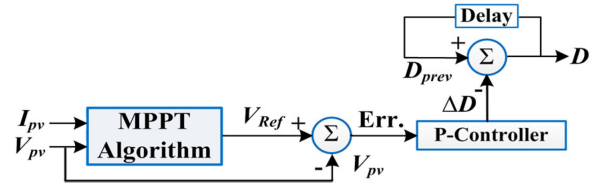


Fig. 2. Proposed D-modulation control scheme.

- 4) Compared to proposed controllers in the past, the proposed method exhibits better performance, and still it is cost effective and easier to implement.

II. D-MODULATION CONTROL SCHEMES

A typical I–V curve of the PV array is shown in Fig. 1. A boost converter is installed between PV array and load. The D of the converter is used as a control variable to regulate the V_{pv} of array. Ideally, it can be evaluated that when D of the converter is set at 1, the switch behaves like a short circuit. Consequently, V_{pv} and I_{pv} of PV array become organized at 0 V and I_{sc} respectively. This relation between D and V_{pv} can be seen in Fig. 1. On the other hand, when D becomes equal to 0, PV array works at open-circuit voltage. Hence, the operational range of modulation index of D always occurs between 0 and 1 i.e., $0 < D < 1$.

The working principle of the proposed PWM controller is shown in Fig. 2. This control scheme is expressed in mathematical form as:

$$D = D_{prev} - \Delta D = D_{prev} - k \times \text{error} \quad (1)$$

where, D_{prev} is the duty cycle of previous iteration and $\Delta D = k \times \text{error} = k \times (V_{Ref} - V_{pv})$. Expression (1) indicates that ideally, D becomes equal to D_{prev} when the magnitude of error is zero. This shows that the proposed scheme holds the ability of integral controller and does not produce any steady-state oscillations when error is zero. Moreover, k gain becomes active only when there is an error. The principle involved in the proposed scheme is mathematically explained with the help of Fig. 1. It can be seen that $V_{Ref} = V_{mpp}$ can be attained, if D is equal to 0.3. Consider that initial D_{in} is 0.22, due to which the PV array is operating at point A. At this point, error is negative

because $V_{pv} (= V_A)$ is greater than V_{Ref} . Therefore, for the next iteration, (1) transforms as:

$$D = D_{prev} - \Delta D = 0.22 + k \times \text{error} \quad (2)$$

It means that if error is negative, ΔD produces a positive impact in D . This situation can be seen from Fig. 1 that in order to achieve MPP from point A, an increase in D value is needed. On the other hand, consider that initial D_{in} is set at 0.45, consequently PV array is operating at point B. Since error is positive in this case as $V_{pv} (= V_B)$ is less than V_{Ref} , therefore (1) can be expressed as:

$$D = D_{prev} - \Delta D = 0.45 - k \times \text{error} \quad (3)$$

Expression (3) indicates that ΔD produces a negative impact in D with positive error, which is required to transfer PV array from point B to MPP. From this debate, it is deduced that a PWM controller based on P-controller philosophy, can be modified to suit the MPP application of PV array. Nevertheless, the optimization (gain setting) of this controller needs to be investigated according to the PV array and load.

III. GAIN SETTING OF D-MODULATION CONTROLLER

In this section, k gain is designed for both resistive and battery loads and a comprehensive study is presented. Although the tuning of k gain has been accomplished with regard to boost converter, this procedure can be used for other converters to set k gain. Expression (1), which describes the working principle of proposed scheme, can be re-written as:

$$D = D_{prev} - k \times \text{error} = D_{prev} - k (V_{Ref} - V_{pv}) \quad (4)$$

Under initial condition, i.e., $t = 0$, the above equation is modified as:

$$D_{mpp} = D_{t=0} - k (V_{Ref} - V_{pv,t=0}) \quad (5)$$

The above expression can be viewed as currently PV array is operating with $D_{t=0}$ and it will reach V_{Ref} point in the next iteration through optimum duty cycle (D_{mpp}). For that, k gain is a vital factor. To obtain it, consider D is initially set at 1 i.e., $D_{t=0} = 1$. As a result, the operating point of PV array becomes settled at short-circuit condition. Therefore, by putting $V_{pv,t=0} = 0$ in (5)

$$D_{mpp} = 1 - k \times V_{Ref} \quad (6)$$

$$k = \frac{1 - D_{mpp}}{V_{Ref}} \quad (7)$$

A. Tuning of k for Resistive Load

Since V_{Ref} will be provided by the algorithm, k gain can be estimated from (7) provided D_{mpp} is known. To obtain D_{mpp} , consider the voltage transfer function of a boost converter:

$$V_o = \frac{1}{1 - D} V_{in} \quad (8)$$

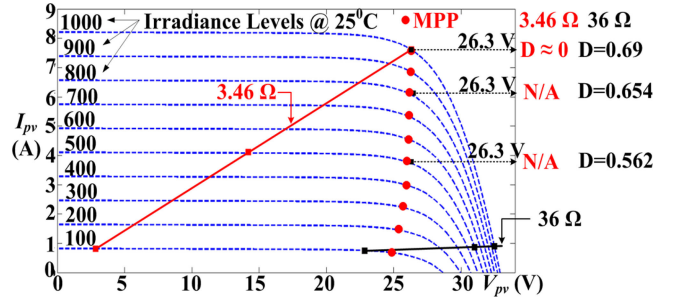


Fig. 3. Profile of resistive load against PV array at distinct irradiance levels.

Assuming the ideal efficiency of converter i.e., $P_{out} = P_{in}$:

$$V_o I_o = V_{in} I_{in} \Rightarrow \frac{V_o^2}{R_o} = \frac{V_{in}^2}{R_{in}} \quad (9)$$

$$R_o = \frac{1}{(1 - D)^2} R_{in} \Rightarrow R_L = \frac{1}{(1 - D)^2} R_{pv_seen} \quad (10)$$

Above relation can be transferred into MPP parameters as:

$$R_L = \frac{1}{(1 - D_{mpp})^2} \times \frac{V_{mpp}}{I_{mpp}} \quad (11)$$

$$D_{mpp} = 1 - \sqrt{\frac{V_{mpp}}{I_{mpp}} \times \frac{1}{R_L}} \quad (12)$$

where, V_{mpp} is equivalent to V_{Ref} . Putting D_{mpp} value from (12) into (7) with $V_{mpp} = V_{Ref}$, the k value can be found out as:

$$k = \frac{\sqrt{\frac{V_{Ref}}{I_{mpp}} \times \frac{1}{R_L}}}{V_{Ref}} = \frac{1}{\sqrt{V_{Ref} \times I_{mpp} \times R_L}} \quad (13)$$

To set the k gain from (13), three parameters are required: 1) V_{Ref} : it is provided by the algorithm, 2) R_L : it can be calculated from the load, and 3) I_{mpp} : it needs to be estimated, if not provided by the algorithm.

For comprehensive analysis, consider Fig. 3 where the I-V curves of Kyocera-200GT module [26] have been generated under different irradiance levels using the PV model given in [27]. Besides that, load lines of two resistances 3.46 Ω and 36 Ω are simulated and superimposed on the I-V curves. Critical observations can be depicted from Fig. 3, which are:

- 1) To obtain V_{Ref} equal to 26.3 V at 1000 W/m² -25 °C, the D_{mpp} value is nearly 0 for 3.46 Ω load and 0.69 for 36 Ω load. It implies that the tuning formula of k gain should contain resistive factor, which can be confirmed from (13).
- 2) Taking 36 Ω resistance into account only, the D_{mpp} values for different weather conditions to obtain the same $V_{Ref} = 26.3$ V are as follows: 0.69 at 1000 W/m², 0.654 at 800 W/m² and 0.562 at 500 W/m². Although a slight change in V_{mpp} value happens with different irradiance levels, same V_{mpp} has been selected for simplicity of analysis. It can be concluded that using the same load resistance and reference voltage, D_{mpp} changes with different irradiance conditions. Thus, k gain should contain the adaptive factor, in which irradiance is reflected. Since

I_{mpp} is mainly influenced by change in irradiance, (13) takes the I_{mpp} factor into account while estimating the gain k .

- 3) According to array size and dc-dc converter, load resistance (R_L) requires calibration. It can be observed from the load profile of 3.46Ω in Fig. 3 that MPP point of only 1000 W/m^2 is achievable. While for other conditions, MPP points are out of scope. On the other hand, almost all MPP points can be achieved with 36Ω . To calibrate R_L , a new formula is developed, the details of which are explained in next section.

I_{mpp} Estimation: Sometimes, MPPT algorithm estimates the values of both V_{Ref} ($= V_{mpp}$) and I_{Ref} ($= I_{mpp}$). The proposed scheme, though asks the V_{Ref} value from the designer. However, it calculates the I_{mpp} value itself, if it is not provided by the designer. For that, the proposed scheme evaluates the present V_{pv} value. If V_{pv} is less than V_{Ref} , it means that PV array is operating in constant-current region where $I_{pv} \approx I_{sc}$. As well-known, I_{mpp} can be estimated from $0.9 \times I_{sc}$, the proposed technique utilizes the same estimation. Therefore, k gain can be calculated from (13) as:

$$k = \frac{1}{\sqrt{V_{Ref} \times 0.9 \times I_{pv} \times R_L}} \quad (14)$$

If $V_{pv} > V_{Ref}$, it means that PV array is in the slope region. In this scenario, the proposed MPPT uses the *Slope* formula for I_{mpp} calculation. With V_{pv} and I_{pv} operating in slope region, the *Slope* between open-circuit point ($V_{oc}, 0$) and present operating point (V_{pv}, I_{pv}) is expressed as:

$$Slope_1 = \frac{0 - I_{pv}}{V_{oc} - V_{pv}} \quad (15)$$

Similarly, the two-point *Slope* relation between open-circuit point ($V_{oc}, 0$) and MPP point (V_{mpp}, I_{mpp}) is written as:

$$Slope_2 = \frac{0 - I_{mpp}}{V_{oc} - V_{mpp}} \quad (16)$$

Consider two slopes are equal i.e., $Slope_1 \approx Slope_2$, (15) and (16) can be equated to find I_{mpp} as:

$$I_{mpp} = \frac{I_{pv}(V_{oc} - V_{mpp})}{V_{oc} - V_{pv}} = \frac{I_{pv}(V_{oc} - V_{Ref})}{V_{oc} - V_{pv}} \quad (17)$$

Substituting I_{mpp} from (17) in (13), k can be found out as:

$$k = \frac{\sqrt{V_{oc} - V_{pv}}}{\sqrt{V_{Ref} \times I_{pv}(V_{oc} - V_{Ref}) \times R_L}} \quad (18)$$

where to estimate k from (14) or (18), I_{pv} and V_{pv} of present point are assessed from sensors, V_{Ref} comes from the designer, while V_{oc} is taken from the manufacturer's datasheet. In case of significant temperature change, the designer may also provide V_{oc} value. Otherwise, it can be updated by using the famous relation V_{Ref}/K , where factor K can be calculated from STC data of datasheet i.e., V_{mpp_STC}/V_{oc_STC} . Finally, the outline of working flowchart of D scheme is:

- 1) Obtain V_{Ref} from MPPT algorithm
- 2) Store present D value i.e., $D_{t=0}$ & then Goto 3
- 3) Is $V_{pv} \approx V_{Ref} \Rightarrow$ Yes: Goto End, No: Goto 4

- 4) Is $V_{pv} < V_{Ref} \Rightarrow$ Yes: Set k from (14) & then Goto 5
 \Rightarrow No: Set k from (18) & then Goto 5
- 5) Set D_{mpp} from (5) & then Goto 6
- 6) Wait for sampling period & then Goto 3

The above steps show that the k gain is calculated during every iteration and it may vary from one weather condition to another. Thus, making k dynamic for resistive load.

R_L Estimation: So far, the criterion to set k gain is explained with regard to constant load. However, in case of load variation, R_L can be estimated from (10) and extra computation step can be merged in the above flowchart. For instance, during each iteration, I_{pv} and V_{pv} of present point are measured from sensors, and last used value of D is fetched from the memory of processing device, therefore (10) can be transformed to calculate R_L as:

$$R_L = \frac{1}{(1 - D)^2} \times \frac{V_{pv}}{I_{pv}} \quad (19)$$

B. Tuning of k for Battery Load

To compute k gain for battery load from (7), D_{mpp} is required. For that, consider the voltage relation of boost converter as ideal battery offers very low impedance:

$$V_B = \frac{1}{1 - D} V_{pv} \Rightarrow V_B = \frac{1}{1 - D_{mpp}} V_{mpp} \quad (20)$$

Using (20), D_{mpp} can be calculated as:

$$D_{mpp} = 1 - \frac{V_{mpp}}{V_B} \quad (21)$$

where, V_{mpp} is equal to V_{Ref} . Substituting D_{mpp} from (21) in (7) with $V_{mpp} = V_{Ref}$, k for battery load can be configured from:

$$k = \frac{1 - \left(1 - \frac{V_{Ref}}{V_B}\right)}{V_{Ref}} = \frac{1}{V_B} \quad (22)$$

The above expression indicates that unlike resistive load, k gain for battery load is static with regard to varying irradiance conditions, and only battery voltage is needed to set the gain.

V_B Estimation: Instead of measuring V_B of battery, the proposed controller estimates V_B through (20). Before every new iteration, the controller updates V_B by taking the information of V_{pv} (from sensor) and D (from memory) of the present operating point. This also incorporates the variations in battery voltage.

For comprehensive analysis, load lines of two battery loads (24 V & 32 V) against different irradiance levels are presented in Fig. 4. Similar to resistive load, Kyocera-200GT module [26] and model [27] are used to generate I-V curves and load lines. Few observations can be noticed from Fig. 4:

- 1) In order to obtain $V_{Ref} = 26.3 \text{ V}$ at different irradiance levels of 1000 W/m^2 , 800 W/m^2 and 500 W/m^2 against the battery load of 32 V, value of D_{mpp} is virtually the same i.e., 0.111. Since an ideal battery has low internal impedance, it accepts the current whatever is provided by the PV array. Consequently, slope of battery load is approximately straight as change in irradiance levels does not produce any significant impact. This concludes that k gain for battery load is static.

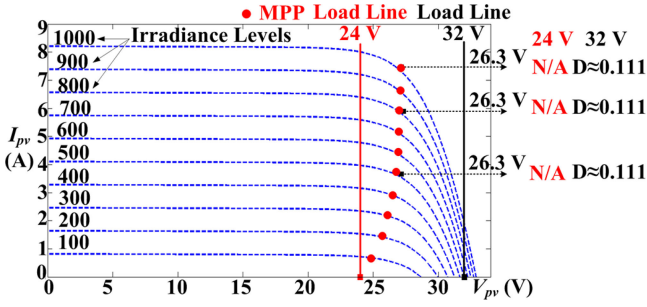


Fig. 4. Profile of battery load against PV array at distinct irradiance levels.

- 2) In order to obtain all the MPPs under different weather conditions, battery load should be calibrated according to array size and converter type. For instance, all the MPP points are out of reach with the battery load of 24 V. A criterion is proposed for the configuration of battery load, which is explained in the next section.

The discussion in this section indicates that the tuning relations of resistive load are different from battery load, as two loads produce distinct duty cycle values for the same operating point of PV array. Therefore, the correlation between gain settings of the two loads is not present.

The principle operation and tuning relations of proposed controller contain parameters according to array size. Therefore, this controller is applicable to any array size. The proposed controller based on battery load can also be applied to grid-connected PV systems, where the input side (DC-link) of inverter behaves as a voltage source.

C. Boundary Limits of Linear Modulation Index

The modulation index of D of converter should occur between 0 & 1, otherwise PV system may become unstable. This implies that:

- 1) Lower Limit (LL): $D = 1 \Rightarrow$ PV array is at: $V_{pv} = 0$ & $I_{pv} = I_{sc}$.
- 2) Upper limit (UL): $D = 0 \Rightarrow$ PV array is at: $V_{pv} = V_{oc}$ & $I_{pv} = 0$.

The scheme presented in this paper provides the facility to check these limits at every iteration. Before assigning the new D , MPPT designer can check the boundary limits from the following two limit relations:

$$LL : 1 = D_{prev} - k \times \text{error} \quad (23)$$

$$UL : 0 = D_{prev} - k \times \text{error} \quad (24)$$

The above expressions are obtained from (1). Expressions (23) and (24) indicate that, once k is computed and D_{prev} is taken from memory, the designer can estimate the magnitude of errors that drag the D to limits.

IV. SIZING OF LOAD VALUES

For the sizing of resistive load, expression (11) of boost converter is used, which indicates that the maximum value of V_{pv} corresponds to $D = 0$. Therefore, (11) transforms into simple

ohms's law relation as:

$$R_L = \frac{V_{mpp}}{I_{mpp}} = \frac{V_{mpp,STC}}{I_{mpp,STC}} \quad (25)$$

Using (25), R_L can be acquired from STC data. However, this implies that V_{mpp} is achievable only if PV array is operating under STC condition or better than STC. At conditions lower than STC, V_{mpp} is out of range due to low I_{mpp} . This phenomenon can be observed from the load line of 3.46Ω (STC) in Fig. 3. A new relation is designed to configure the R_L , which is expressed in (26). It is based on a simple reason that V_{mpp} value of STC condition should be attained even irradiance falls to 100 W/m^2 . Since I_{mpp} of 100 W/m^2 is not present in the datasheet, 10% I_{mpp} of STC is selected.

$$R_L = \frac{V_{mpp,STC}}{10\% \times I_{mpp,STC}} \quad (26)$$

As voltage is influenced by temperature change, a more concise formula to set resistive load is:

$$R_L = \frac{V_{mpp,STC} + k_v (T_{MIN} - 25^\circ\text{C})}{10\% \times I_{mpp,STC}} \quad (27)$$

The above expression indicates that resistive load should be calibrated with minimum temperature (T_{MIN}) of the location where PV plant is installed. It is because of the reason that k_v is the negative temperature coefficient of V_{oc} of module. k_v can be extracted from the datasheet while for T_{MIN} , meteorological data of winter season of the location can be consulted.

For battery load, the change in irradiance does not produce any significant impact. Therefore, expression (20) can be used to calibrate the battery load, where maximum value of V_{pv} corresponds to zero value of D . Hence V_{pv} becomes equal to V_B . Since MPP points occur upto $0.8-0.85 V_{oc,STC}$, the battery load is set at $0.95 V_{oc,STC}$.

$$V_B = 0.95 \times V_{oc,STC} \quad (28)$$

Because V_{oc} is affected by the temperature change, a more comprehensive formula to set the battery load is:

$$V_B = 0.95 \times (V_{oc,STC} + k_v (T_{MIN} - 25^\circ\text{C})) \quad (29)$$

V. SIMULATION STUDY AND COMPARATIVE ANALYSIS

Using the comprehensive PV array model [27], D-modulation schemes are implemented in Matlab/Simulink to analyze the comparative performance. PV array is comprised of four PV modules arranged in 2×2 series-parallel configuration. Each module belongs to FVG 36-125 (50166) [28]. Boost converter is connected between the PV array and load. The components values of boost converter are: $C_{in} = 150 \mu\text{F}$, $C_{out} = 250 \mu\text{F}$ and $L = 300 \mu\text{H}$. The switching frequency of converter is set at 40 kHz , while sampling rate of PV system is settled at 5 ms .

A. Resistive Load

In case of resistive load, performance of three control schemes is evaluated. These are: 1) Proposed controller (D_{prop}), 2) MPPT (D [2]), and Perturb and Observe (P&O) method. As already

TABLE I
PERFORMANCE OF CONTROLLERS AGAINST TWO LOADS

| Type of Load | Performance of Controllers | D_{prop} | D [2] | P&O – 0.04 | P&O – 0.05 | P&O – 0.07 | PID |
|----------------|----------------------------|---|---|---|---|--|--|
| Resistive Load | Convergence Time | $(4 + 1) \times 5 \text{ ms} = 25 \text{ ms}$ | $(6 + 3) \times 5 \text{ ms} = 45 \text{ ms}$ | $(6 + 4) \times 5 \text{ ms} = 50 \text{ ms}$ | - | - | - |
| Battery Load | Convergence Time | $(2 + 1) \times 5 \text{ ms} = 15 \text{ ms}$ | $(13 + 8) \times 5 \text{ ms} = 105 \text{ ms}$ | $(18 + 6) \times 5 \text{ ms} = 120 \text{ ms}$ | $(16 + 4) \times 5 \text{ ms} = 100 \text{ ms}$ | $(14 + 3) \times 5 \text{ ms} = 85 \text{ ms}$ | $(3 + 16) \times 5 \text{ ms} = 95 \text{ ms}$ |
| | Energy (J) | 51.3 | 44.8 | 40.7 | 42.3 | 42.6 | 41.3 |

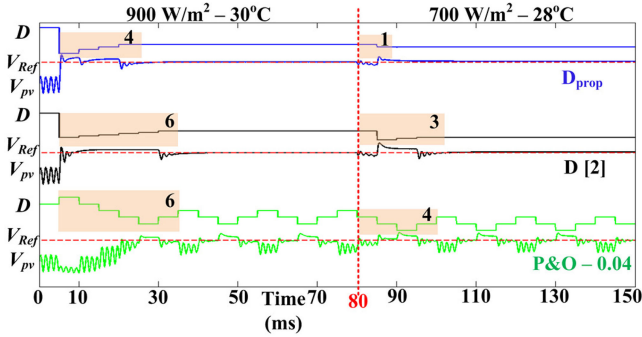


Fig. 5. Performance of controllers under resistive load.

described, k gain is computed at every iteration during the operation of D_{prop} . The gain is determined from (14) if $V_{pv} < V_{Ref}$ or from (18) if $V_{pv} > V_{Ref}$. The working principle of D [2] is based on two main operations: first it utilizes the special D relation to set PV array in close vicinity of V_{Ref} , and then employs the incremental conductance (IC) method to reach MPP accurately. P&O is a classical method that works with a ΔD of 0.04. Using (27), R_L is set at 47Ω . Comparison between techniques has been carried out with regard to following factors:

Tracking ability: All control schemes have been programmed with an initial duty cycle of 0.75. At first, the behavior of each scheme is examined under $900 \text{ W/m}^2 - 30^\circ\text{C}$, where $V_{Ref} = 35.5 \text{ V}$ is given to each control scheme. After 80 ms, the schemes are subject to step fall of $700 \text{ W/m}^2 - 28^\circ\text{C}$. Under this condition, the MPPT algorithm provides $V_{Ref} = 35.8 \text{ V}$ to control schemes. Fig. 5 shows the tracking ability of each controller, which indicates that during initial condition, the proposed scheme (blue line) maneuvers D four times to set V_{pv} at reference point. After the change in weather condition at 80 ms, the performance of D_{prop} is enhanced as it consumes just one sample to attain V_{Ref} . Both D [2] and P&O process six samples during initial condition, whereas D [2] executes less samples when a step change is observed in weather conditions.

The relative performance of every method is tabulated in Table I, which indicates that the convergence speed of D_{prop} is almost twice of D [2] and P&O. Thus, it confirms the working principle and tuning criteria of the D_{prop} .

Number of tuning parameters and tuning criteria: Each controller contains single tuning parameter. However, D_{prop} comes with one-step tuning relation. Both D [2] and P&O fail to provide tuning criteria for their respective ΔD factors that deal with variations in size of PV array and distinct loads.

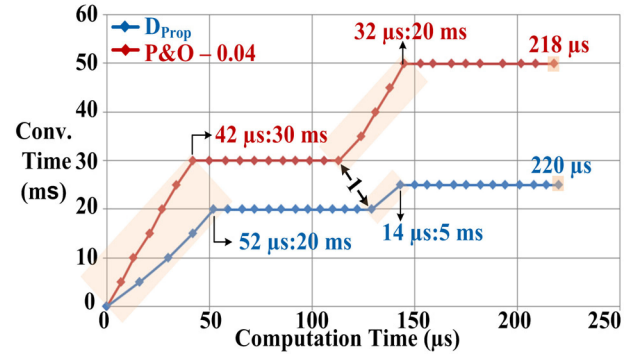


Fig. 6. Convergence time vs Computation time between D_{prop} and P&O.

Sensors required and computation complexity: In terms of sensors requirement, all methods are equally matched as they use both current and voltage sensors. On the other hand, the computation complexity of P&O is lowest as its algorithm contains few *if-else* branches and moderate D relations. Whereas numerous conditional statements, complex fractions, and square root relations make the computation burden of D [2], the highest. The complexity of D_{prop} is average as given by the algorithm steps in Section III; however, it becomes less complex when V_{Ref} is achieved as single *if* statement is processed. To elaborate the matter, Fig. 6 shows the graph between convergence time vs computation time (C_{p-t}) of D_{prop} and P&O. The graph is generated according to the results presented in Fig. 5. The instruction execution time of processing unit is $1 \mu\text{s}$. It can be seen from Fig. 6 that D_{prop} takes 20 ms to reach V_{Ref} , and in the process it conceives an average computation time (C_{p-t}) of $13 \mu\text{s}$ for 4 samples. The execution of (14)/(18) is behind the higher C_{p-t} of D_{prop} . In comparison, P&O takes 30 ms to reach optimal point, and consumes an average C_{p-t} of $7 \mu\text{s}$ for 6 samples.

For entire time range, the total C_{p-t} of proposed method is $220 \mu\text{s}$, which is very close to total $C_{p-t} = 218 \mu\text{s}$ of P&O. It is because of two reasons: 1) once the steady-state is achieved, C_{p-t} of D_{prop} is vastly reduced to $5\text{--}6 \mu\text{s/sample}$ as the algorithm only checks $V_{pv} \approx V_{Ref}$ condition, and 2) it just consumes one sample with $C_{p-t} = 14 \mu\text{s}$ to achieve the V_{Ref} when condition changes as indicated by Arrow-1 in Fig. 6. By contrast, P&O executes the same sets of subroutines whether in dynamic or steady state, hence its C_{p-t} remains the same. Consequently, for the entire range, D_{prop} manages similar computation time as that of P&O. Nevertheless, the proposed method requires a processing unit that must be equipped with sophisticated arithmetic logic unit (ALU).

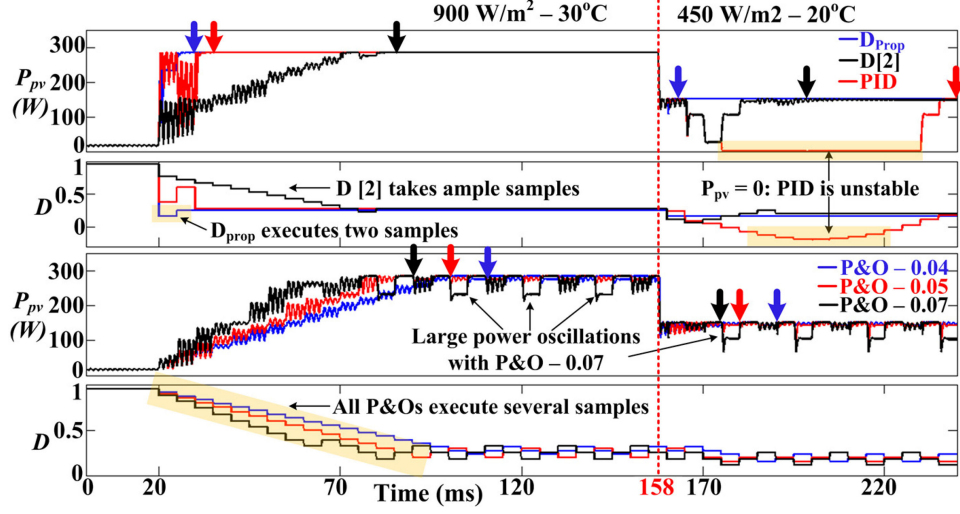


Fig. 7. P_{pv} and D of control schemes under battery load.

B. Battery Load

For battery load, proportional integral differential (PID) controller is also included along with schemes compared in previous section. The PID controller is optimized with $k_p = 0.005$, $k_i = 0.5$ and $k_d = 0.00005$. The same simulation setup of resistive load is used, except the load is changed with battery. The value of which is set at 48 V through (29). For D_{prop} , the k gain is initially calculated as 0.021 from (22). Afterwards, it is updated before every new iteration.

Tracking ability: All D -schemes are started with D_{in} of 0.95. Initially, methods are tested under $900 \text{ W/m}^2 - 30^\circ\text{C}$. During this condition, $V_{Ref} = 35.5 \text{ V}$ is sent to D -schemes by the MPPT algorithm. After that, PV array is subject to step fall of $450 \text{ W/m}^2 - 20^\circ\text{C}$ at 158 ms and new reference voltage of 38.1 V is forwarded to the schemes.

Upper two graphs of Fig. 7 indicate the tracking ability of D_{prop} , $D[2]$ and PID in the context of P_{pv} and D iterations, whereas lower two graphs show the same for P&O with different step sizes. The arrows with respective colors of schemes indicate the accomplishment of MPP tracking. Upper D graph illustrates that D_{prop} consumes two samples during initial condition, and it takes one sample to achieve V_{Ref} , when condition changes at 158 ms.

As far as other schemes are concerned, PID is the only scheme which matches the performance of D_{prop} during initial condition. However, it becomes unstable and sets inappropriate negative D values when weather takes the step fall as indicated in Fig. 7. This highlights that adequate gain setting is required for different conditions.

All other schemes take ample samples to set the PV array at V_{Ref} as indicated by arrows shown in Fig. 7. Especially, the performance of $D[2]$ decays significantly for battery load as compared to resistive load. The relative performance of each method is tabulated in Table I, which clearly indicates that in terms of energy yield, D_{prop} outcores other methods by a significant margin. The data specify that D_{prop} is the only method

which extracts energy more than 50 J, while other schemes hover around in the range of 40 to 45 J.

Amongst P&O, the algorithm with 0.07 step size, has the fastest convergence time as indicated in Table I. However, it exhibits large power loss oscillations compared to other P&O algorithms with smaller step sizes. From a long term perspective, P&O-0.05 exhibits a good tradeoff between convergence speed and steady oscillations, as it yields similar energy to P&O-0.07. Since D_{prop} executes few samples under battery load, P&O with any step size struggles to match the performance of D_{prop} , which can be confirmed from Table I as well as from Fig. 7. Note that if there is a significant difference between the current D and optimum D , P&O struggles because of its one-dimensional approach. For instance, during initial condition, P&O has to travel from $D_{in} = 0.95$ to almost other extreme, i.e., $D_{in} = 0.2$. While D_{prop} covers such a difference of D through its robust controller and consumes only two samples.

No of tuning parameters and tuning criteria: All control schemes contain single tuning parameter except PID controller, which contains three parameters. With the exception of D_{prop} , other techniques failed to provide any significant criteria for setting gains.

Sensors required and computation complexity: D_{prop} and PID schemes require only voltage sensing in their respective operations. While $D[2]$ and P&O require both V_{pv} and I_{pv} sensors. Therefore, D_{prop} is more cost effective.

In terms of complexity, $D[2]$ and PID schemes are more complex. The computation complexity of D_{prop} is less than its resistive counterpart and its computation time is even better than P&O. Note that under battery load, algorithm of D_{prop} needs to process a moderate relation (22) and two conditional statements. In addition, its dynamic performance is better.

Fig. 8 shows the curves according to results presented in Fig. 7. During initial condition, D_{prop} has convergence time of 10 ms, and it executes two samples with C_{p-t} of $12 \mu\text{s}$. After that, it simply processes the conditional statement of $V_{pv} \approx V_{Ref}$.

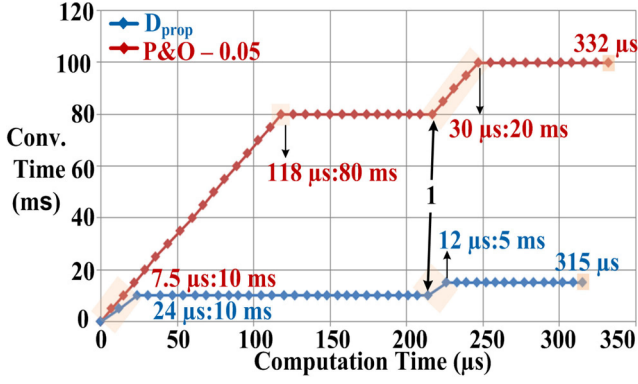


Fig. 8. Convergence time vs Computation time between D_{prop} and P&O.

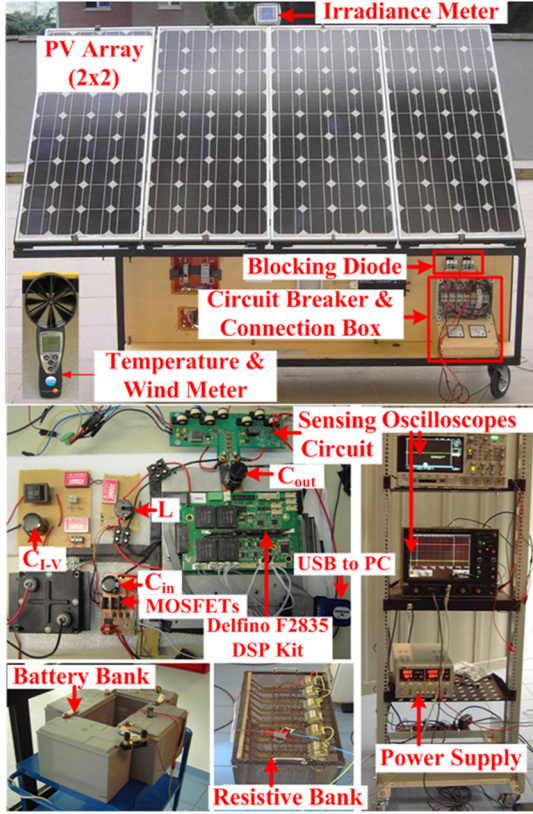


Fig. 9. Experimental bench setup containing mobile PV array.

When weather changes at Arrow-1 position, D_{prop} consumes C_{p-t} of 12 μs for single sample only.

Contrary to resistive load, P&O struggles significantly compared to D_{prop} in terms of convergence speed as evident from the gap present between algorithm's curves in Fig. 8. The reason behind inept performance of P&O is to reach far away optimum D values from present D value. At the same time, computation burden of P&O is high as it exhibits total C_{p-t} of 332 μs compared to C_{p-t} = 315 μs of D_{prop} .

VI. EXPERIMENTAL SETUP, RESULTS AND DISCUSSIONS

All devices of experimental setup along with labels are shown in Fig. 9. The setup is organized in the same way as that of

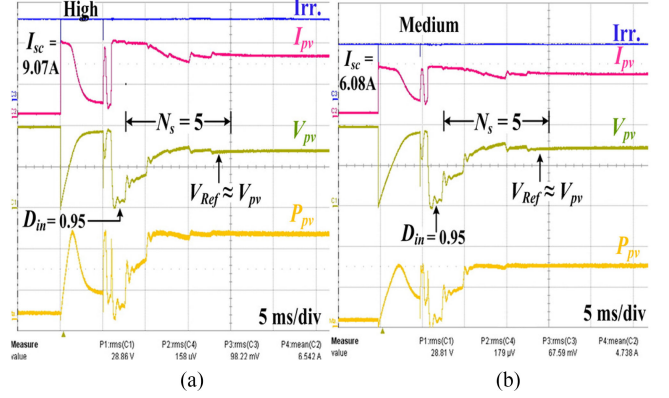


Fig. 10. Performance of proposed controller under resistive load.

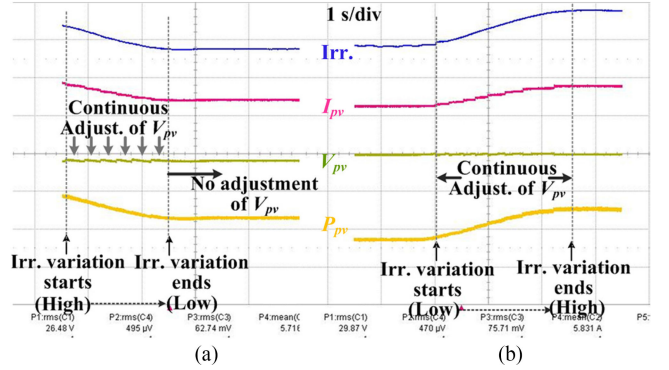


Fig. 11. Response of proposed controller under varying weather conditions.

simulation setup. PV array is installed on mobile cart. I-V curve tracer based MPPT [3] is used to detect the MPP point. For that, a capacitor of 1 mF is installed in the setup.

Fig. 10(a) and Fig. 10(b) illustrate the standard format of experimental tests. Initially, algorithm [3] disengages the array from load and then I-V curve is scanned to detect the MPP variables. After that, algorithm sends V_{mpp} value as a reference voltage (V_{Ref}) to the proposed scheme and PV array is re-connected with load. Initial value of D is set at 0.95 and the role of D_{prop} is to set the operating point of PV array at V_{Ref} by modulating the D of converter.

A. Resistive Load

A resistive load of 47 Ω is connected, which is calculated through (27). k gain of proposed controller is adjusted during each iteration as mentioned in Section III. Fig. 10(a) and Fig. 10(b) depict high irradiance (I_{sc} = 9.12 A) and medium irradiance (I_{sc} = 6.08 A) conditions, respectively. Under both conditions, D_{prop} executes five samples to set the array at V_{Ref} .

Another dynamic test is conducted as shown in Fig. 11(a), where the PV array is faced towards the sun. Then, it is moved away from the sun using the mobile cart. This can be confirmed from the fall in irradiance signal as shown in Fig. 11(a). Under this condition, proposed method adjusts D in an effective way and always operates the array near V_{Ref} . On the other hand, Fig. 11(b) shows that PV array is moved back towards the sun as indicated by irradiance sensor. The continuous operation of

TABLE II
TUNING RELATIONS FOR BUCK AND BUCK-BOOST CONVERTER

| Converter | | Resistive | | Battery |
|------------|-------------------------------|---|---|---|
| | | $k =$ | | $k =$ |
| | | $V_{pv} < V_{Ref}$ | $V_{pv} > V_{Ref}$ | |
| Buck | | $\frac{\left(1 - \sqrt{\frac{R_L \times 0.9 \times I_{pv}}{V_{Ref}}}\right)}{V_{Ref} - V_{out}}$ | $\left(1 - \sqrt{\frac{R_L \times I_{pv} \times (V_{oc} - V_{Ref})}{V_{Ref} \times (V_{oc} - V_{pv})}}\right) \frac{1}{V_{Ref} - V_{out}}$ | $\frac{1}{V_{Ref}}$ |
| Buck-Boost | Buck Mode $V_o < V_{Ref}$ | $\frac{\left(0.5 - \frac{\sqrt{R_L}}{\sqrt{\frac{V_{Ref}}{0.9 \times I_{pv}} + \sqrt{R_L}}}\right)}{V_{Ref} - V_{out}}$ | $\left(0.5 - \frac{\sqrt{R_L}}{\sqrt{\frac{V_{Ref} \times (V_{oc} - V_{pv})}{I_{pv} \times (V_{oc} - V_{Ref})} + \sqrt{R_L}}}\right) \frac{1}{V_{Ref} - V_{out}}$ | $\frac{0.5 \times (V_B + V_{Ref}) - V_B}{(V_B + V_{Ref}) \times (V_{Ref} - V_B)}$ |
| | Boost Mode $V_o > V_{Ref}$ | $\frac{1}{V_{Ref} + \sqrt{V_{Ref} \times R_L \times 0.9 \times I_{pv}}}$ | $\frac{1}{V_{Ref} + \sqrt{V_{Ref} \times R_L \times I_{pv} \times \frac{(V_{oc} - V_{Ref})}{(V_{oc} - V_{pv})}}}$ | $\frac{1}{V_B + V_{Ref}}$ |

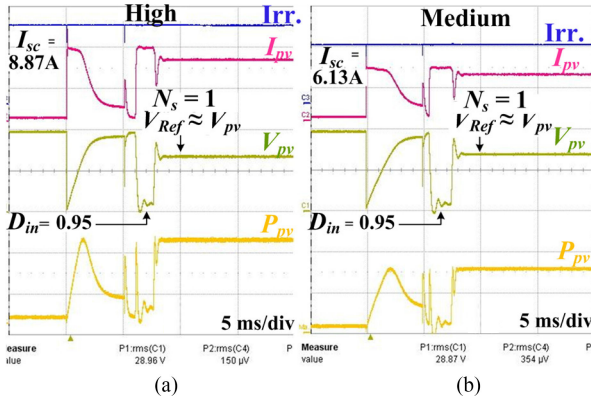


Fig. 12. Response of proposed controller under battery load.

array near V_{Ref} confirms the efficient operation of D_{prop} scheme. Hence, these experimental tests validate not only the principle operation of proposed scheme, but also verify the tuning relation of k gain.

B. Battery Load

A battery load of 48 V is interfaced at the output of the converter. k gain of D_{prop} is set at 0.021 using (22), and afterwards it is updated during every iteration. Fig. 12(a) and Fig. 12(b) illustrate the high irradiance and medium irradiance conditions, respectively. Initially, capacitor scanning based algorithm [3] traces the I-V curve and transfers V_{mpp} value to D_{prop} . It can be seen from Fig. 12 that the proposed scheme takes single sample to adjust D during both conditions. These results exhibit strong similarity to simulation results.

In another test, PV array is partially shaded. In this case, a specialized MPPT algorithm [29] is used to track the global maximum. For that, algorithm [29] calculates four voltage points, and then sends these four V_{Ref} values to D_{prop} . Fig. 13 shows that after receiving four reference values, the proposed scheme

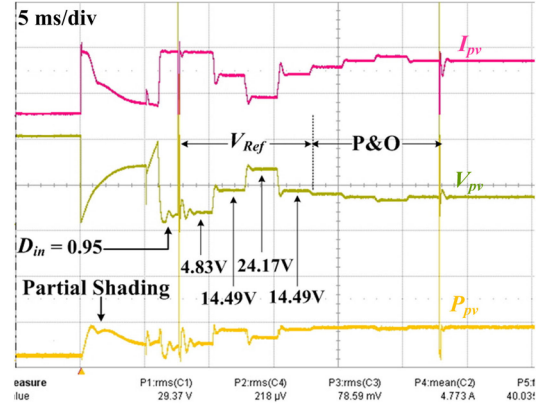


Fig. 13. Response of proposed controller under partial shading.

requires a single iteration to set the V_{pv} at each V_{Ref} value, thus verifying the effectiveness of the proposed scheme. After that, algorithm [29] executes the P&O method to reach the GM precisely.

VII. CONCLUSION

In this paper, two vital aspects of PV system are addressed. A pulse width modulation (PWM) controller is presented, whose working principle holds the ability of integral controller and it utilizes only single tuning parameter. A comprehensive study is presented to design k gain of the proposed controller. It is revealed that k gain should be dynamic for resistive load, while it can be static for battery load with regard to weather conditions. Using the single step gain relations, the PWM controller is auto-tuned during each iteration. Compared to previously proposed PWM schemes, the proposed scheme has the following advantages: 1) it is low cost, 2) tuning criteria are provided to set the k gain for both resistive and battery loads, and 3) high tracking ability is obtained. The proposed controller also exhibits similar computation time as that of basic perturb and observe algorithm,

nevertheless it requires a processing device with sophisticated arithmetic logic unit. Moreover, two new expressions have been proposed for the sizing of load values according to boost converter. With such load values, MPPT controller can reach MPP points even under low irradiance conditions.

In the end, the tuning relations of gain k for other two popularly used converters in PV systems are featured in Table II.

REFERENCES

- [1] J.-H. Teng, W.-H. Huang, T.-A. Hsu, and C.-Y. Wang, "Novel and fast maximum power point tracking for photovoltaic generation," *IEEE Trans. Ind. Electron.*, vol. 63, no. 8, pp. 4955–4966, Apr. 2016.
- [2] T. K. Soon and S. Mekhilef, "A Fast-converging MPPT technique for photovoltaic system under Fast-Varying solar irradiation and Load resistance," *IEEE Trans. Energy Convers.*, vol. 11, no. 1, pp. 176–186, Feb. 2015.
- [3] F. Spertino, J. Ahmad, A. Ciocia, P. Di Leo, A. F. Murtaza, and M. Chiaberge, "Capacitor charging method for I–V curve tracer and MPPT in photovoltaic systems," *Solar Energy*, vol. 119, pp. 461–473, Sep. 2015.
- [4] M. Sokolov and D. Shmilovitz, "A Modified MPPT scheme for accelerated convergence," *IEEE Trans. Energy Convers.*, vol. 23, no. 4, pp. 1105–1107, Dec. 2008.
- [5] C. Manickam, G. R. Raman, G. P. Raman, S. I. Ganesan, and C. Nagamani, "A Hybrid Algorithm for Tracking of GMPP Based on P&O and PSO with reduced power oscillation in string inverters," *IEEE Trans. Ind. Electron.*, vol. 63, no. 10, pp. 6097–6106, Jul. 2016.
- [6] X. Fan, F. Deng, and J. Chen, "Voltage band analysis for maximum power point tracking of stand-alone PV systems," *Solar Energy*, vol. 144, pp. 221–231, Mar. 2017.
- [7] R. Balasankar, G. T. Arasu, and J. S. C. Mano, "A global MPPT technique invoking partitioned estimation and strategic deployment of P&O to tackle partial shading conditions," *Solar Energy*, vol. 143, pp. 73–85, Feb. 2017.
- [8] H. Patel and V. Agarwal, "Maximum power point tracking scheme for PV systems operating under partially shaded conditions," *IEEE Trans. Ind. Electron.*, vol. 55, no. 4, pp. 1689–1698, Apr. 2008.
- [9] J. Ahmed and Z. Salam, "A maximum power point tracking (MPPT) for PV system using cuckoo search with partial shading capability," *Appl. Energy*, vol. 119, pp. 118–130, Apr. 2014.
- [10] M. A. Ghasemi, H. M. Forushani, and M. Parniani, "Partial shading detection and smooth maximum power point tracking of PV arrays under PSC," *IEEE Trans. Power Electron.*, vol. 31, no. 9, pp. 6281–6292, Sep. 2016.
- [11] J. Ahmed, S. Member, and Z. Salam, "An improved method to predict the position of maximum power point during partial shading for PV Arrays," *IEEE Trans. Ind. Informat.*, vol. 11, no. 6, pp. 1378–1387, Dec. 2015.
- [12] M. H. Moradi and A. R. Reisi, "A hybrid maximum power point tracking method for photovoltaic systems," *Solar Energy*, vol. 85, no. 11, pp. 2965–2976, Nov. 2011.
- [13] J. S. C. M. Raj and A. E. Jeyakumar, "A novel maximum power point tracking technique for photovoltaic module based on power plane analysis of I–V characteristics," *IEEE Trans. Ind. Electron.*, vol. 61, no. 9, pp. 4734–4745, Sep. 2014.
- [14] F. Zhang, K. Thanapalan, A. Procter, S. Carr, and J. Maddy, "Adaptive hybrid maximum power point tracking method for a photovoltaic system," *IEEE Trans. Energy Convers.*, vol. 28, no. 2, pp. 353–360, Jun. 2013.
- [15] R. Pradhan and B. Subudhi, "Design and real-time implementation of a new auto-tuned adaptive MPPT control for a photovoltaic system," *Int. J. Electr. Power Energy Syst.*, vol. 64, pp. 792–803, Jan. 2015.
- [16] L. Corradini, P. Mattavelli, W. Stefanutti, and S. Saggini, "Simplified model reference-based autotuning for digitally controlled SMPS," *IEEE Trans. Power Electron.*, vol. 23, no. 4, pp. 1956–1963, Jul. 2008.
- [17] S. Saggini, W. Stefanutti, E. Tedeschi, and P. Mattavelli, "Digital deadbeat control tuning for dc–dc converters using error correlation," *IEEE Trans. Power Electron.*, vol. 22, no. 4, pp. 1566–1570, Jul. 2007.
- [18] M. Shirazi, R. Zane, and D. Maksimovic, "An autotuning digital controller for DC–DC power converters based on online frequency-response measurement," *IEEE Trans. Power Electron.*, vol. 24, no. 11, pp. 2578–2588, Nov. 2009.
- [19] R. N. Tripathi and T. Hanamoto, "Two degrees of freedom dc voltage controller of grid interfaced PV system with optimized gains," *Int. J. Electr. Power Energy Syst.*, vol. 85, pp. 87–96, 2017.
- [20] E. I. Batzelis, G. E. Kampitsis, and S. A. Papathanassiou, "Power reserves control for PV systems with real-time MPP estimation via curve fitting," *IEEE Trans. Sustain. Energy*, vol. 8, no. 3, pp. 1269–1280, Jul. 2017.
- [21] M. Sitbon, S. Schacham, and A. Kuperman, "Disturbance observer based voltage regulation of current-mode-boost-converter-interfaced photovoltaic generator," *IEEE Trans. Ind. Electron.*, vol. 62, no. 9, pp. 5776–5785, Sep. 2015.
- [22] R. Errouissi, A. Al-Durra, and S. M. Mueeen, "A robust continuous-time MPC of a DC–DC boost converter interfaced with a grid-connected photovoltaic system," *IEEE J. Photovolt.*, vol. 6, no. 6, pp. 1619–1629, Aug. 2016.
- [23] D. R. Espinoza-Trejo, E. Bárcenas-Bárcenas, D. U. Campos-Delgado, and C. H. De Angelo, "Voltage-oriented input-output linearization controller as maximum power point tracking technique for photovoltaic systems," *IEEE Trans. Ind. Electron.*, vol. 62, no. 6, pp. 3499–3507, Nov. 2014.
- [24] K. Dezelak, P. Bracinik, M. Höger, and A. Otcenasova, "Comparison between the particle swarm optimization and differential evolution approaches for the optimal proportional-integral controllers design during photovoltaic power plants modelling," *IET Renew. Power Gener.*, vol. 10, no. 4, pp. 522–530, Mar. 2016.
- [25] A. I. Dounis, P. Kofinas, G. Papadakis, and C. Alafodimos, "A direct adaptive neural control for maximum power point tracking of photovoltaic system," *Solar Energy*, vol. 115, pp. 145–165, May 2015.
- [26] [Online]. Available: <http://www.kyocera.com.sg/products/solar/pdf/kc200gt.pdf>. Accessed on: Jan. 2017.
- [27] M. G. Villalva, J. R. Gazoli, and E. R. Filho, "Comprehensive approach to modeling and simulation of photovoltaic arrays," *IEEE Trans. Power Electron.*, vol. 24, no. 5, pp. 1198–1208, May 2009.
- [28] [Online]. Available: http://www.yeint.fi/files/products/FVG36_125_ENG.pdf. Accessed on: Jan. 2017.
- [29] A. Murtaza, M. Chiaberge, F. Spertino, D. Boero, and M. De Giuseppe, "A maximum power point tracking technique based on bypass diode mechanism for PV arrays under partial shading," *Energy Buildings*, vol. 73, pp. 13–25, Apr. 2014.

